

Asymptotic Postbuckling Analysis of Composite and Sandwich Structures via the Assumed Strain Solid Shell Element Formulation

Jihan Kim¹, Yong Hyup Kim¹ and Sung Won Lee²

Abstract: The Koiter's asymptotic method is combined with the assumed strain solid shell element formulation for postbuckling analysis of composite and sandwich structures. The assumed strain solid shell element is free of locking and the small angle assumption, and it allows multiple plies through the element thickness. While laminated composite structures are modeled with single element through the thickness, sandwich structures are modeled with three elements stacked through the thickness to model the face sheets and the core independently. The Koiter's method is used to trace initial postbuckling path. Subsequently, the Koiter's method is switched to the arc-length method to investigate postbuckling behavior involving large deflections. The transition point at which the switching occurs is determined using the postbuckling coefficients, obtained from the asymptotic analysis with the fourth order expansion. Numerical tests demonstrate the validity and effectiveness of the present approach.

keyword: Koiter's method; buckling and postbuckling; finite element formulation; assumed strain solid shell element formulation; composite sandwich plates; transition point.

1 Introduction

Structural components are often subjected to compressive loading, and they must be designed against buckling. However, buckling does not necessarily mean that a structure cannot resist additional load above the initial buckling load. For example, a column or a thin plate can take additional compressive load as they bend further. Accordingly, one of the important considerations for structural integrity is the buckling and postbuckling behavior.

The postbuckling analysis can be conducted by using the

branch switching followed by a nonlinear analysis such as the arc-length method [Hao, Cho, and Lee (2000)]. Alternately, the asymptotic method such as the Koiter's method [Byskov and Hutchinson (1977)] can be used for initial postbuckling analysis. When the Koiter's method was incorporated within the context of the finite element method, problems have arisen in the calculation of the second-order postbuckling coefficient. The locking effect was identified as the cause, and researches have been conducted to resolve the problems observed in simple frame structures, beams and isotropic plates.

Structural analyses can be often carried out by using solid shell elements [Lee, Cho, and Lee (2002)] or plate elements [Glaessgen, Riddell, and Raju (2002)]. In this paper, the assumed strain solid shell element formulation is combined with the Koiter's method for postbuckling analysis of isotropic, composite and sandwich structures. The formulation for the assumed strain solid shell element has been introduced and verified for composite structures by Kim and Lee (1988). The assumed strain formulation introduces independently assumed strain field at an element level in addition to the assumed displacement to alleviate element locking. The added assumed strain parameters are eliminated at the element level, leaving the nodal displacements as the degrees of freedom as in the case of the assumed displacement formulation. The solid shell element is attractive in that it does not use any rotational angles as degrees of freedom. The kinematics of deformation is described by purely vectorial variables, and large deflection problems can be solved without adopting the small angle assumption. Also, the solid shell element can be easily stacked through the thickness. Accordingly, it is convenient for the analysis of sandwich structures with composite face-sheets and a core.

The Koiter's method is used to trace initial postbuckling path of composite plates and sandwich plates. However, in order to investigate subsequent behavior, the Koiter's

¹ Seoul National University, Seoul, Korea

² University of Maryland, College Park, MD, U.S.A

method is switched to nonlinear analysis using the arc-length method [Clarke and Hancock (1990)]. The transition point at which the switching occurs is determined using the postbuckling coefficients, obtained from the asymptotic analysis with the fourth order expansion. Numerical tests are conducted to demonstrate the validity and effectiveness of the present approach. Example problems include composite and sandwich structures. For sandwich structures, the interaction between the stiff face sheets and flexible core may have significant influence on the initial postbuckling path and the subsequent postbuckling behavior. Accordingly, the postbuckling behaviors of sandwich plates with various core densities are investigated.

2 Formulation

In this section the assumed strain formulation of the Koiter's method is introduced. For a solid in equilibrium,

$$\int_V \delta \bar{\boldsymbol{\epsilon}}^T \cdot \boldsymbol{\sigma} dV - \delta W = 0 \quad (1)$$

where $\delta \bar{\boldsymbol{\epsilon}}$ is the virtual strain vector, $\boldsymbol{\sigma}$ is the second Piola-Kirchhoff stress vector, δW is the external virtual work due to applied load and V is the volume. The external virtual work can be expressed as

$$\delta W = \lambda \delta \mathbf{u}^T \cdot \mathbf{R} \quad (2)$$

where λ is the load parameter, $\delta \mathbf{u}$ is the virtual nodal displacement vector and \mathbf{R} is the reference load vector. For the assumed strain formulation, an independent strain field is introduced in addition to the displacement-dependent strain field. The compatibility between the independent strain vector $\boldsymbol{\epsilon}$ and the displacement-dependent strain vector $\bar{\boldsymbol{\epsilon}}$ can be expressed as

$$\int_V \delta \boldsymbol{\epsilon}^T \mathbf{C} (\boldsymbol{\epsilon} - \bar{\boldsymbol{\epsilon}}) dV = 0 \quad (3)$$

where $\delta \boldsymbol{\epsilon}$ is the virtual independent strain vector and $\boldsymbol{\epsilon}$ is the virtual independent strain vector. The stress vector is related to the independent strain vector as follows:

$$\boldsymbol{\sigma} = \mathbf{C} \boldsymbol{\epsilon} \quad (4)$$

where \mathbf{C} is the 6×6 elastic constitutive matrix. In a manner consistent with the kinematics of shell deformation,

the constitutive matrix is constructed such that in-plane normal stresses and transverse normal stress are decoupled to remove undesirable constraints.

The displacement-dependent strain vector $\bar{\boldsymbol{\epsilon}}$ can be related to the nodal displacement vector \mathbf{u} such that

$$\bar{\boldsymbol{\epsilon}} = \mathbf{B} \mathbf{u} + \frac{1}{2} \mathbf{A} (\mathbf{B}' \mathbf{u}, \mathbf{B}' \mathbf{u}) \quad (5)$$

In equation (5), the first term represents a linear strain and the second term is a nonlinear strain. The \mathbf{B} is a matrix relates $\bar{\boldsymbol{\epsilon}}$ and \mathbf{u} linearly, \mathbf{B}' is a matrix relating the displacement vector and its derivatives with respect to each coordinates and the \mathbf{A} -operator represents a nonlinear Green strain in terms of displacement vector.

In the Koiter's method, the deformation path is divided into two segments; the prebuckling path and the postbuckling path as shown in Fig. 1. The prebuckling path is assumed linear in the present study.

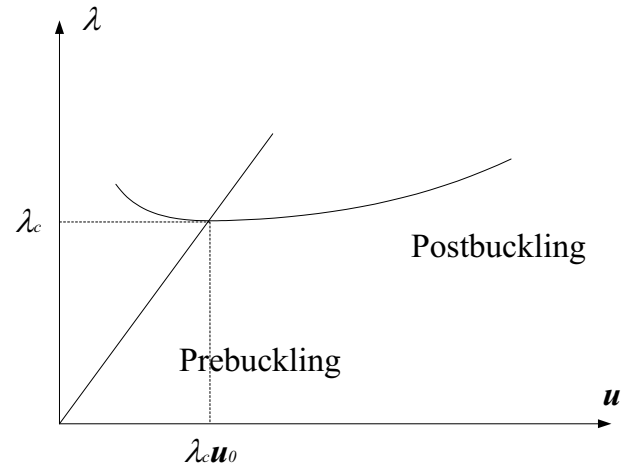


Figure 1 : Asymptotic paths of prebuckling and postbuckling

In the postbuckling region, the nodal displacement field \mathbf{u} and load parameter λ are expanded into the perturbation series in terms of the buckling amplitude (or expansion parameter) ξ as follows:

$$\mathbf{u} = \lambda \mathbf{u}_0 + \mathbf{u}_1 \xi + \mathbf{u}_2 \xi^2 + \mathbf{u}_3 \xi^3 + \mathbf{u}_4 \xi^4 + \dots \quad (6)$$

$$\frac{\lambda}{\lambda_c} = 1 + a \xi + b \xi^2 + c \xi^3 + d \xi^4 + \dots \quad (7)$$

where \mathbf{u}_0 is the displacement field with respect to the unit load vector \mathbf{R} , \mathbf{u}_1 is the buckling mode, \mathbf{u}_2 is second order

displacement field, \mathbf{u}_3 is third order displacement field, \mathbf{u}_4 is fourth order displacement field, λ_c is the buckling load and a , b , c and d are the postbuckling coefficients. In this section the fourth order expansion of the Koiter's method is formulated.

The displacement-dependent strain vector can then be expressed as follows:

$$\bar{\boldsymbol{\varepsilon}} = \lambda \bar{\boldsymbol{\varepsilon}}_0 + \bar{\boldsymbol{\varepsilon}}_1 \xi + \bar{\boldsymbol{\varepsilon}}_2 \xi^2 + \bar{\boldsymbol{\varepsilon}}_3 \xi^3 + \bar{\boldsymbol{\varepsilon}}_4 \xi^4 + \dots \quad (8)$$

where

$$\begin{aligned} \bar{\boldsymbol{\varepsilon}}_0 &= \mathbf{B}\mathbf{u}_0 \\ \bar{\boldsymbol{\varepsilon}}_1 &= \mathbf{B}\mathbf{u}_1 \\ \bar{\boldsymbol{\varepsilon}}_2 &= \mathbf{B}\mathbf{u}_2 + \frac{1}{2}A(\mathbf{B}'\mathbf{u}_1, \mathbf{B}'\mathbf{u}_1) \\ \bar{\boldsymbol{\varepsilon}}_3 &= \mathbf{B}\mathbf{u}_3 + A(\mathbf{B}'\mathbf{u}_1, \mathbf{B}'\mathbf{u}_2) \\ \bar{\boldsymbol{\varepsilon}}_4 &= \mathbf{B}\mathbf{u}_4 + A(\mathbf{B}'\mathbf{u}_1, \mathbf{B}'\mathbf{u}_3) + \frac{1}{2}A(\mathbf{B}'\mathbf{u}_2, \mathbf{B}'\mathbf{u}_2) \end{aligned} \quad (9)$$

The independently assumed strain vector $\boldsymbol{\varepsilon}$ is expressed in terms of the assumed parameter vector $\boldsymbol{\alpha}$ such that

$$\boldsymbol{\varepsilon} = \mathbf{P}\boldsymbol{\alpha} \quad (10)$$

where \mathbf{P} is a matrix of assumed strain shape functions. The assumed parameter vector can also be written in an expanded form as

$$\boldsymbol{\alpha} = \lambda \boldsymbol{\alpha}_0 + \boldsymbol{\alpha}_1 \xi + \boldsymbol{\alpha}_2 \xi^2 + \boldsymbol{\alpha}_3 \xi^3 + \boldsymbol{\alpha}_4 \xi^4 + \dots \quad (11)$$

Placing equation (11) into equation (10),

$$\boldsymbol{\varepsilon} = \lambda \boldsymbol{\varepsilon}_0 + \boldsymbol{\varepsilon}_1 \xi + \boldsymbol{\varepsilon}_2 \xi^2 + \boldsymbol{\varepsilon}_3 \xi^3 + \boldsymbol{\varepsilon}_4 \xi^4 + \dots \quad (12)$$

where

$$\begin{aligned} \boldsymbol{\varepsilon}_0 &= \mathbf{P}\boldsymbol{\alpha}_0 \\ \boldsymbol{\varepsilon}_1 &= \mathbf{P}\boldsymbol{\alpha}_1 \\ \boldsymbol{\varepsilon}_2 &= \mathbf{P}\boldsymbol{\alpha}_2 \\ \boldsymbol{\varepsilon}_3 &= \mathbf{P}\boldsymbol{\alpha}_3 \\ \boldsymbol{\varepsilon}_4 &= \mathbf{P}\boldsymbol{\alpha}_4 \end{aligned} \quad (13)$$

Substituting equations (5)~(13) to equation (3), one can find the relationships between the assumed strain parameters and element nodal displacement vectors as follows:

$$\begin{aligned} \boldsymbol{\alpha}_0 &= \mathbf{H}^{-1}\mathbf{G}\mathbf{u}_0 \\ \boldsymbol{\alpha}_1 &= \mathbf{H}^{-1}\mathbf{G}\mathbf{u}_1 \\ \boldsymbol{\alpha}_2 &= \mathbf{H}^{-1}[\mathbf{G}\mathbf{u}_2 + \frac{1}{2}\mathbf{P}^T\mathbf{C}A(\mathbf{B}'\mathbf{u}_1, \mathbf{B}'\mathbf{u}_1)] \\ \boldsymbol{\alpha}_3 &= \mathbf{H}^{-1}[\mathbf{G}\mathbf{u}_3 + \mathbf{P}^T\mathbf{C}A(\mathbf{B}'\mathbf{u}_1, \mathbf{B}'\mathbf{u}_2)] \\ \boldsymbol{\alpha}_4 &= \mathbf{H}^{-1}[\mathbf{G}\mathbf{u}_4 + \mathbf{P}^T\mathbf{C}[A(\mathbf{B}'\mathbf{u}_1, \mathbf{B}'\mathbf{u}_3) \\ &\quad + \frac{1}{2}A(\mathbf{B}'\mathbf{u}_2, \mathbf{B}'\mathbf{u}_2)]] \end{aligned} \quad (14)$$

where $\mathbf{H} = \int_{V_e} \mathbf{P}^T \mathbf{C} \mathbf{P} dV$, $\mathbf{G} = \int_{V_e} \mathbf{P}^T \mathbf{C} \mathbf{B} dV$.

Note that equation (14) holds at element level, and the integrations are carried out over element volume V_e .

All defined fields and obtained fields can be substituted to the equilibrium equation (1) and can be reduced. The reduced equation can be divided into different orders in terms of ξ as follows:

2.1 The zero-order problem

The equation for the zero-order problem is expressed as

$$\mathbf{G}^T \mathbf{H}^{-1} \mathbf{G} \mathbf{u}_0 = \mathbf{K} \mathbf{u}_0 = \mathbf{R} \quad (15)$$

where \mathbf{K} is the linear stiffness matrix of the assumed strain formulation.

2.2 The first-order problem

The first-order problem is a linear eigenvalue problem with the equation expressed as

$$\begin{aligned} &[\mathbf{G}^T \mathbf{H}^{-1} \mathbf{G} + \lambda_c \int_V \mathbf{B}'^T \mathbf{S}_0 \mathbf{B}' dV] \mathbf{u}_1 \\ &= [\mathbf{K} + \lambda_c \mathbf{K}_s] \mathbf{u}_1 = 0 \end{aligned} \quad (16)$$

where \mathbf{K}_s is the initial stress stiffness matrix, \mathbf{S}_0 is the matrix with initial stress ($\boldsymbol{\sigma}_0$) components.

The \mathbf{S}_i matrix is related to the i^{th} order stress vector ($\boldsymbol{\sigma}_i$) such that

$$\boldsymbol{\sigma}_i^T A(\mathbf{B}'\mathbf{u}_j, \mathbf{B}'\mathbf{u}_k) = \mathbf{u}_j^T \mathbf{B}'^T \mathbf{S}_i \mathbf{B}' \mathbf{u}_k \quad (17)$$

where $\boldsymbol{\sigma}_i = \mathbf{C}\boldsymbol{\varepsilon}_i = \mathbf{C}\mathbf{P}\boldsymbol{\alpha}_i$.

2.3 The second-order problem

The equations for the second-order problem are

$$\begin{aligned} &[\mathbf{K} + \lambda_c \mathbf{K}_s] \mathbf{u}_2 \\ &= - \int_V [\mathbf{B}'^T (a\lambda_c \mathbf{S}_0 + \mathbf{S}_1) \mathbf{B}' \mathbf{u}_1] dV \\ &\quad - \int_V [\mathbf{G}^T \mathbf{H}^{-1} \frac{1}{2} \mathbf{P}^T \mathbf{C} A(\mathbf{B}'\mathbf{u}_1, \mathbf{B}'\mathbf{u}_1)] dV \end{aligned} \quad (18)$$

$$\mathbf{u}_1^T \mathbf{K} \mathbf{u}_2 = 0 \quad (19)$$

The left hand side of the equation (18) is similar to the one of the first order problem and equation (18) is singular. To resolve this, equation (19) is added. To determine postbuckling constant a , one may premultiply equation (18) with \mathbf{u}_1^T such that

$$\begin{aligned} &\mathbf{u}_1^T [\mathbf{K} + \lambda_c \mathbf{K}_s] \mathbf{u}_2 \\ &= - \int_V [\mathbf{u}_1^T \mathbf{B}'^T (a\lambda_c \mathbf{S}_0 + \mathbf{S}_1) \mathbf{B}' \mathbf{u}_1] dV \\ &\quad - \int_V [\mathbf{u}_1^T \mathbf{G}^T \mathbf{H}^{-1} \frac{1}{2} \mathbf{P}^T \mathbf{C} A(\mathbf{B}'\mathbf{u}_1, \mathbf{B}'\mathbf{u}_1)] dV \end{aligned} \quad (20)$$

The left hand side of equation (20) is equal to zero, and the right hand side (RHS) of equation (20) can be expressed as

$$\begin{aligned}
 &RHS \\
 &= - \int_V [\mathbf{u}_1^T \mathbf{B}'^T (a\lambda_c \mathbf{S}_0 + \mathbf{S}_1) \mathbf{B}' \mathbf{u}_1] dV \\
 &\quad - \int_V [\boldsymbol{\alpha}_1^T \frac{1}{2} \mathbf{P}^T \mathbf{C} \mathbf{A} (\mathbf{B}' \mathbf{u}_1, \mathbf{B}' \mathbf{u}_1)] dV \\
 &= - \int_V [\mathbf{u}_1^T \mathbf{B}'^T (a\lambda_c \mathbf{S}_0 + \mathbf{S}_1) \mathbf{B}' \mathbf{u}_1] dV \\
 &\quad - \int_V [\frac{1}{2} \boldsymbol{\sigma}_1^T \mathbf{A} (\mathbf{B}' \mathbf{u}_1, \mathbf{B}' \mathbf{u}_1)] dV \\
 &= - \int_V [\mathbf{u}_1^T \mathbf{B}'^T (a\lambda_c \mathbf{S}_0 + \mathbf{S}_1) \mathbf{B}' \mathbf{u}_1] dV \\
 &\quad - \int_V [\frac{1}{2} \mathbf{u}_1^T \mathbf{B}'^T \mathbf{S}_1 \mathbf{B}' \mathbf{u}_1] dV \\
 &= - \int_V [a\lambda_c \mathbf{u}_1^T \mathbf{B}'^T \mathbf{S}_0 \mathbf{B}' \mathbf{u}_1] dV \\
 &\quad - \int_V [\frac{3}{2} \mathbf{u}_1^T \mathbf{B}'^T \mathbf{S}_1 \mathbf{B}' \mathbf{u}_1] dV \\
 &= 0
 \end{aligned} \tag{21}$$

From equation (21),

$$a\lambda_c = - \frac{3 \mathbf{u}_1^T [\int_V \mathbf{B}'^T \mathbf{S}_1 \mathbf{B}' dV] \mathbf{u}_1}{2 \mathbf{u}_1^T [\int_V \mathbf{B}'^T \mathbf{S}_0 \mathbf{B}' dV] \mathbf{u}_1} \tag{22}$$

where \mathbf{S}_1 is the matrix with the first order stress ($\boldsymbol{\sigma}_1$) components similar to \mathbf{S}_0 . The postbuckling coefficient a is expressed by \mathbf{u}_0 and \mathbf{u}_1 which are known fields. Accordingly, the postbuckling coefficient a can be calculated using equation (22) before solving the second order problem. Subsequently, the second order displacement field \mathbf{u}_2 can be obtained by solving equation (18) and (19) simultaneously. Note that the right hand side of the second order problem can be written in a single vector form, and the solution procedure for the second order problem is almost same as that for a linear problem.

2.4 The third-order problem

The equations for the third-order problem are

$$\begin{aligned}
 &[\mathbf{K} + \lambda_c \mathbf{K}_s] \mathbf{u}_3 \\
 &= - \int_V [\mathbf{B}'^T (a\lambda_c \mathbf{S}_0 + \mathbf{S}_1) \mathbf{B}' \mathbf{u}_2] dV \\
 &\quad - \int_V [\mathbf{B}'^T (b\lambda_c \mathbf{S}_0 + \mathbf{S}_2) \mathbf{B}' \mathbf{u}_1] dV \\
 &\quad - \int_V [\mathbf{G}^T \mathbf{H}^{-1} \mathbf{P}^T \mathbf{C} \mathbf{A} (\mathbf{B}' \mathbf{u}_1, \mathbf{B}' \mathbf{u}_2)] dV
 \end{aligned} \tag{23}$$

$$\mathbf{u}_1^T \mathbf{K} \mathbf{u}_3 = 0 \tag{24}$$

The orthogonality condition between \mathbf{u}_1 and \mathbf{u}_3 shown in equation (24) is added to avoid singularity. Premultiply-

ing equation (23) with \mathbf{u}_1^T ,

$$\begin{aligned}
 &\mathbf{u}_1^T [\mathbf{K} + \lambda_c \mathbf{K}_s] \mathbf{u}_3 \\
 &= - \int_V [\mathbf{u}_1^T \mathbf{B}'^T (a\lambda_c \mathbf{S}_0 + \mathbf{S}_1) \mathbf{B}' \mathbf{u}_2] dV \\
 &\quad - \int_V [\mathbf{u}_1^T \mathbf{B}'^T (b\lambda_c \mathbf{S}_0 + \mathbf{S}_2) \mathbf{B}' \mathbf{u}_1] dV \\
 &\quad - \int_V [\mathbf{u}_1^T \mathbf{G}^T \mathbf{H}^{-1} \mathbf{P}^T \mathbf{C} \mathbf{A} (\mathbf{B}' \mathbf{u}_1, \mathbf{B}' \mathbf{u}_2)] dV
 \end{aligned} \tag{25}$$

The left hand side of equation (25) is equal to zero. Accordingly,

$$\begin{aligned}
 &RHS \\
 &= - \int_V [\mathbf{u}_1^T \mathbf{B}'^T (a\lambda_c \mathbf{S}_0 + \mathbf{S}_1) \mathbf{B}' \mathbf{u}_2] dV \\
 &\quad - \int_V [\mathbf{u}_1^T \mathbf{B}'^T (b\lambda_c \mathbf{S}_0 + \mathbf{S}_2) \mathbf{B}' \mathbf{u}_1] dV \\
 &\quad - \int_V [\boldsymbol{\alpha}_1^T \mathbf{P}^T \mathbf{C} \mathbf{A} (\mathbf{B}' \mathbf{u}_1, \mathbf{B}' \mathbf{u}_2)] dV \\
 &= - \int_V [\mathbf{u}_1^T \mathbf{B}'^T (a\lambda_c \mathbf{S}_0 + \mathbf{S}_1) \mathbf{B}' \mathbf{u}_2] dV \\
 &\quad - \int_V [\mathbf{u}_1^T \mathbf{B}'^T (b\lambda_c \mathbf{S}_0 + \mathbf{S}_2) \mathbf{B}' \mathbf{u}_1] dV \\
 &\quad - \int_V [\boldsymbol{\sigma}_1^T \mathbf{A} (\mathbf{B}' \mathbf{u}_1, \mathbf{B}' \mathbf{u}_2)] dV \\
 &= - \int_V [\mathbf{u}_1^T \mathbf{B}'^T (a\lambda_c \mathbf{S}_0 + \mathbf{S}_1) \mathbf{B}' \mathbf{u}_2] dV \\
 &\quad - \int_V [\mathbf{u}_1^T \mathbf{B}'^T (b\lambda_c \mathbf{S}_0 + \mathbf{S}_2) \mathbf{B}' \mathbf{u}_1] dV \\
 &\quad - \int_V [\mathbf{u}_1^T \mathbf{B}'^T \mathbf{S}_1 \mathbf{B}' \mathbf{u}_2] dV \\
 &= - \int_V [a\lambda_c \underbrace{\mathbf{u}_1^T \mathbf{B}'^T \mathbf{S}_0 \mathbf{B}' \mathbf{u}_2}_{=0 \text{ from eq. (16) \& (19)}}] dV \\
 &\quad - \int_V [\mathbf{u}_1^T \mathbf{B}'^T (b\lambda_c \mathbf{S}_0 + \mathbf{S}_2) \mathbf{B}' \mathbf{u}_1] dV \\
 &\quad - \int_V [2\mathbf{u}_1^T \mathbf{B}'^T \mathbf{S}_1 \mathbf{B}' \mathbf{u}_2] dV \\
 &= - \int_V [b\lambda_c \mathbf{u}_1^T \mathbf{B}'^T \mathbf{S}_0 \mathbf{B}' \mathbf{u}_1] dV \\
 &\quad - \int_V [\mathbf{u}_1^T \mathbf{B}'^T \mathbf{S}_2 \mathbf{B}' \mathbf{u}_1] dV \\
 &\quad - \int_V [2\mathbf{u}_1^T \mathbf{B}'^T \mathbf{S}_1 \mathbf{B}' \mathbf{u}_2] dV \\
 &= 0
 \end{aligned} \tag{26}$$

From equation (26), one obtains the equation to determine the postbuckling coefficient b as follows:

$$b\lambda_c = - \frac{\mathbf{u}_1^T [\int_V \mathbf{B}'^T \mathbf{S}_2 \mathbf{B}' dV] \mathbf{u}_1}{\mathbf{u}_1^T [\int_V \mathbf{B}'^T \mathbf{S}_0 \mathbf{B}' dV] \mathbf{u}_1} - \frac{2\mathbf{u}_1^T [\int_V \mathbf{B}'^T \mathbf{S}_1 \mathbf{B}' dV] \mathbf{u}_2}{\mathbf{u}_1^T [\int_V \mathbf{B}'^T \mathbf{S}_0 \mathbf{B}' dV] \mathbf{u}_1} \tag{27}$$

where \mathbf{S}_2 is the matrix with the second order stress ($\boldsymbol{\sigma}_2$) components similar to \mathbf{S}_0 and \mathbf{S}_1 .

2.5 The fourth-order problem

The fourth-order problem is similar to the second and the third order problems. The fourth order displacement field

\mathbf{u}_4 can be calculated from the following two equations.

$$\begin{aligned} & [\mathbf{K} + \lambda_c \mathbf{K}_s] \mathbf{u}_4 \\ &= - \int_V [\mathbf{B}'^T (a\lambda_c \mathbf{S}_0 + \mathbf{S}_1) \mathbf{B}' \mathbf{u}_3] dV \\ & \quad - \int_V [\mathbf{B}'^T (b\lambda_c \mathbf{S}_0 + \mathbf{S}_2) \mathbf{B}' \mathbf{u}_2] dV \\ & \quad - \int_V [\mathbf{B}'^T (c\lambda_c \mathbf{S}_0 + \mathbf{S}_3) \mathbf{B}' \mathbf{u}_1] dV \\ & \quad - \int_V [\mathbf{G}^T \mathbf{H}^{-1} \mathbf{P}^T \mathbf{C} \mathbf{A} (\mathbf{B}' \mathbf{u}_1, \mathbf{B}' \mathbf{u}_3)] dV \\ & \quad - \int_V [\mathbf{G}^T \mathbf{H}^{-1} \mathbf{P}^T \mathbf{C} \frac{1}{2} \mathbf{A} (\mathbf{B}' \mathbf{u}_2, \mathbf{B}' \mathbf{u}_2)] dV \end{aligned} \quad (28)$$

$$\mathbf{u}_1^T \mathbf{K} \mathbf{u}_4 = 0 \quad (29)$$

Premultiplying equation (28) with \mathbf{u}_1^T ,

$$\begin{aligned} & \mathbf{u}_1^T [\mathbf{K} + \lambda_c \mathbf{K}_s] \mathbf{u}_4 \\ &= - \int_V [\mathbf{u}_1^T \mathbf{B}'^T (a\lambda_c \mathbf{S}_0 + \mathbf{S}_1) \mathbf{B}' \mathbf{u}_3] dV \\ & \quad - \int_V [\mathbf{u}_1^T \mathbf{B}'^T (b\lambda_c \mathbf{S}_0 + \mathbf{S}_2) \mathbf{B}' \mathbf{u}_2] dV \\ & \quad - \int_V [\mathbf{u}_1^T \mathbf{B}'^T (c\lambda_c \mathbf{S}_0 + \mathbf{S}_3) \mathbf{B}' \mathbf{u}_1] dV \\ & \quad - \int_V [\mathbf{u}_1^T \mathbf{G}^T \mathbf{H}^{-1} \mathbf{P}^T \mathbf{C} \mathbf{A} (\mathbf{B}' \mathbf{u}_1, \mathbf{B}' \mathbf{u}_3)] dV \\ & \quad - \int_V [\mathbf{u}_1^T \mathbf{G}^T \mathbf{H}^{-1} \mathbf{P}^T \mathbf{C} \frac{1}{2} \mathbf{A} (\mathbf{B}' \mathbf{u}_2, \mathbf{B}' \mathbf{u}_2)] dV \end{aligned} \quad (30)$$

The left hand side of equation (30) is equal to zero, and thus

RHS

$$\begin{aligned} &= - \int_V [\mathbf{u}_1^T \mathbf{B}'^T (a\lambda_c \mathbf{S}_0 + \mathbf{S}_1) \mathbf{B}' \mathbf{u}_3] dV \\ & \quad - \int_V [\mathbf{u}_1^T \mathbf{B}'^T (b\lambda_c \mathbf{S}_0 + \mathbf{S}_2) \mathbf{B}' \mathbf{u}_2] dV \\ & \quad - \int_V [\mathbf{u}_1^T \mathbf{B}'^T (c\lambda_c \mathbf{S}_0 + \mathbf{S}_3) \mathbf{B}' \mathbf{u}_1] dV \\ & \quad - \int_V [\alpha_1^T \mathbf{P}^T \mathbf{C} \mathbf{A} (\mathbf{B}' \mathbf{u}_1, \mathbf{B}' \mathbf{u}_3)] dV \\ & \quad - \int_V [\alpha_1^T \mathbf{P}^T \mathbf{C} \frac{1}{2} \mathbf{A} (\mathbf{B}' \mathbf{u}_2, \mathbf{B}' \mathbf{u}_2)] dV \\ &= - \int_V [\mathbf{u}_1^T \mathbf{B}'^T (a\lambda_c \mathbf{S}_0 + \mathbf{S}_1) \mathbf{B}' \mathbf{u}_3] dV \\ & \quad - \int_V [\mathbf{u}_1^T \mathbf{B}'^T (b\lambda_c \mathbf{S}_0 + \mathbf{S}_2) \mathbf{B}' \mathbf{u}_2] dV \\ & \quad - \int_V [\mathbf{u}_1^T \mathbf{B}'^T (c\lambda_c \mathbf{S}_0 + \mathbf{S}_3) \mathbf{B}' \mathbf{u}_1] dV \\ & \quad - \int_V [\sigma_1^T \mathbf{A} (\mathbf{B}' \mathbf{u}_1, \mathbf{B}' \mathbf{u}_3)] dV \\ & \quad - \int_V [\sigma_1^T \frac{1}{2} \mathbf{A} (\mathbf{B}' \mathbf{u}_2, \mathbf{B}' \mathbf{u}_2)] dV \\ &= - \int_V [a\lambda_c \underbrace{\mathbf{u}_1^T \mathbf{B}'^T \mathbf{S}_0 \mathbf{B}' \mathbf{u}_3}_{=0 \text{ from eq. (16) \& (24)}} + \mathbf{u}_1^T \mathbf{B}'^T \mathbf{S}_1 \mathbf{B}' \mathbf{u}_3] dV \\ & \quad - \int_V [b\lambda_c \underbrace{\mathbf{u}_1^T \mathbf{B}'^T \mathbf{S}_0 \mathbf{B}' \mathbf{u}_2}_{=0 \text{ from eq. (16) \& (19)}} + \mathbf{u}_1^T \mathbf{B}'^T \mathbf{S}_2 \mathbf{B}' \mathbf{u}_2] dV \\ & \quad - \int_V [c\lambda_c \mathbf{u}_1^T \mathbf{B}'^T \mathbf{S}_0 \mathbf{B}' \mathbf{u}_1 + \mathbf{u}_1^T \mathbf{B}'^T \mathbf{S}_3 \mathbf{B}' \mathbf{u}_1] dV \\ & \quad - \int_V [\mathbf{u}_1^T \mathbf{B}'^T \mathbf{S}_1 \mathbf{B}' \mathbf{u}_3 + \frac{1}{2} \mathbf{u}_2^T \mathbf{B}'^T \mathbf{S}_1 \mathbf{B}' \mathbf{u}_2] dV \\ &= - \int_V [c\lambda_c \mathbf{u}_1^T \mathbf{B}'^T \mathbf{S}_0 \mathbf{B}' \mathbf{u}_1 + \mathbf{u}_1^T \mathbf{B}'^T \mathbf{S}_3 \mathbf{B}' \mathbf{u}_1] dV \\ & \quad - \int_V [\mathbf{u}_1^T \mathbf{B}'^T \mathbf{S}_2 \mathbf{B}' \mathbf{u}_2 + 2\mathbf{u}_1^T \mathbf{B}'^T \mathbf{S}_1 \mathbf{B}' \mathbf{u}_3] dV \\ & \quad - \int_V [\frac{1}{2} \mathbf{u}_2^T \mathbf{B}'^T \mathbf{S}_1 \mathbf{B}' \mathbf{u}_2] dV \\ &= 0 \end{aligned}$$

From equation (31),

$$\begin{aligned} c\lambda_c = & - \frac{\mathbf{u}_1^T [\int_V \mathbf{B}'^T \mathbf{S}_3 \mathbf{B}' dV] \mathbf{u}_1}{\mathbf{u}_1^T [\int_V \mathbf{B}'^T \mathbf{S}_0 \mathbf{B}' dV] \mathbf{u}_1} \\ & - \frac{\mathbf{u}_1^T [\int_V \mathbf{B}'^T \mathbf{S}_2 \mathbf{B}' dV] \mathbf{u}_2}{\mathbf{u}_1^T [\int_V \mathbf{B}'^T \mathbf{S}_0 \mathbf{B}' dV] \mathbf{u}_1} \\ & - \frac{2\mathbf{u}_1^T [\int_V \mathbf{B}'^T \mathbf{S}_1 \mathbf{B}' dV] \mathbf{u}_3}{\mathbf{u}_1^T [\int_V \mathbf{B}'^T \mathbf{S}_0 \mathbf{B}' dV] \mathbf{u}_1} \\ & - \frac{\frac{1}{2} \mathbf{u}_2^T [\int_V \mathbf{B}'^T \mathbf{S}_1 \mathbf{B}' dV] \mathbf{u}_2}{\mathbf{u}_1^T [\int_V \mathbf{B}'^T \mathbf{S}_0 \mathbf{B}' dV] \mathbf{u}_1} \end{aligned} \quad (32)$$

where \mathbf{S}_3 is the matrix with the third order stress (σ_3) components similar to \mathbf{S}_2 . Postbuckling coefficient c can be determined using equation (32).

2.6 The postbuckling coefficient d

To determine the fourth order postbuckling coefficient d , one may look at the following equation corresponding to the fifth-order problem:

$$\begin{aligned} & [\mathbf{K} + \lambda_c \mathbf{K}_s] \mathbf{u}_5 \\ &= - \int_V [\mathbf{B}'^T (a\lambda_c \mathbf{S}_0 + \mathbf{S}_1) \mathbf{B}' \mathbf{u}_4] dV \\ & \quad - \int_V [\mathbf{B}'^T (b\lambda_c \mathbf{S}_0 + \mathbf{S}_2) \mathbf{B}' \mathbf{u}_3] dV \\ & \quad - \int_V [\mathbf{B}'^T (c\lambda_c \mathbf{S}_0 + \mathbf{S}_3) \mathbf{B}' \mathbf{u}_2] dV \\ & \quad - \int_V [\mathbf{B}'^T (d\lambda_c \mathbf{S}_0 + \mathbf{S}_4) \mathbf{B}' \mathbf{u}_1] dV \\ & \quad - \int_V [\mathbf{G}^T \mathbf{H}^{-1} \mathbf{P}^T \mathbf{C} \mathbf{A} (\mathbf{B}' \mathbf{u}_1, \mathbf{B}' \mathbf{u}_4)] dV \\ & \quad - \int_V [\mathbf{G}^T \mathbf{H}^{-1} \mathbf{P}^T \mathbf{C} \mathbf{A} (\mathbf{B}' \mathbf{u}_2, \mathbf{B}' \mathbf{u}_3)] dV \end{aligned} \quad (31)$$

Premultiplying equation (33) with \mathbf{u}_1^T ,

$$\begin{aligned} & \mathbf{u}_1^T [\mathbf{K} + \lambda_c \mathbf{K}_s] \mathbf{u}_5 \\ &= - \int_V [\mathbf{u}_1^T \mathbf{B}'^T (a\lambda_c \mathbf{S}_0 + \mathbf{S}_1) \mathbf{B}' \mathbf{u}_4] dV \\ & \quad - \int_V [\mathbf{u}_1^T \mathbf{B}'^T (b\lambda_c \mathbf{S}_0 + \mathbf{S}_2) \mathbf{B}' \mathbf{u}_3] dV \\ & \quad - \int_V [\mathbf{u}_1^T \mathbf{B}'^T (c\lambda_c \mathbf{S}_0 + \mathbf{S}_3) \mathbf{B}' \mathbf{u}_2] dV \\ & \quad - \int_V [\mathbf{u}_1^T \mathbf{B}'^T (d\lambda_c \mathbf{S}_0 + \mathbf{S}_4) \mathbf{B}' \mathbf{u}_1] dV \\ & \quad - \int_V [\mathbf{u}_1^T \mathbf{G}^T \mathbf{H}^{-1} \mathbf{P}^T \mathbf{C} \mathbf{A} (\mathbf{B}' \mathbf{u}_1, \mathbf{B}' \mathbf{u}_4)] dV \\ & \quad - \int_V [\mathbf{u}_1^T \mathbf{G}^T \mathbf{H}^{-1} \mathbf{P}^T \mathbf{C} \mathbf{A} (\mathbf{B}' \mathbf{u}_2, \mathbf{B}' \mathbf{u}_3)] dV \end{aligned} \quad (34)$$

Then, noting that the left hand side of equation (34) is

equal to zero,

$$\begin{aligned}
 &RHS \\
 &= - \int_V [u_1^T B'^T (a\lambda_c S_0 + S_1) B' u_4] dV \\
 &\quad - \int_V [u_1^T B'^T (b\lambda_c S_0 + S_2) B' u_3] dV \\
 &\quad - \int_V [u_1^T B'^T (c\lambda_c S_0 + S_3) B' u_2] dV \\
 &\quad - \int_V [u_1^T B'^T (d\lambda_c S_0 + S_4) B' u_1] dV \\
 &\quad - \int_V [\alpha_1^T P^T CA(B' u_1, B' u_4)] dV \\
 &\quad - \int_V [\alpha_1^T P^T CA(B' u_2, B' u_3)] dV \\
 &= - \int_V [u_1^T B'^T (a\lambda_c S_0 + S_1) B' u_4] dV \\
 &\quad - \int_V [u_1^T B'^T (b\lambda_c S_0 + S_2) B' u_3] dV \\
 &\quad - \int_V [u_1^T B'^T (c\lambda_c S_0 + S_3) B' u_2] dV \\
 &\quad - \int_V [u_1^T B'^T (d\lambda_c S_0 + S_4) B' u_1] dV \\
 &\quad - \int_V [\sigma_1^T A(B' u_1, B' u_4)] dV \\
 &\quad - \int_V [\sigma_1^T A(B' u_2, B' u_3)] dV \\
 &= - \int_V [a\lambda_c \underbrace{u_1^T B'^T S_0 B' u_4}_{=0 \text{ from eq. (16) \& (29)}} + u_1^T B'^T S_1 B' u_4] dV \\
 &\quad - \int_V [b\lambda_c \underbrace{u_1^T B'^T S_0 B' u_3}_{=0 \text{ from eq. (16) \& (24)}} + u_1^T B'^T S_2 B' u_3] dV \\
 &\quad - \int_V [c\lambda_c \underbrace{u_1^T B'^T S_0 B' u_2}_{=0 \text{ from eq. (16) \& (19)}} + u_1^T B'^T S_3 B' u_2] dV \\
 &\quad - \int_V [d\lambda_c u_1^T B'^T S_0 B' u_1 + u_1^T B'^T S_4 B' u_1] dV \\
 &\quad - \int_V [u_1^T B'^T S_1 B' u_4 + u_2^T B'^T S_1 B' u_3] dV \\
 &= - \int_V [d\lambda_c u_1^T B'^T S_0 B' u_1 + u_1^T B'^T S_4 B' u_1] dV \\
 &\quad - \int_V [u_1^T B'^T S_3 B' u_2 + u_1^T B'^T S_2 B' u_3] dV \\
 &\quad - \int_V [2u_1^T B'^T S_1 B' u_4 + u_2^T B'^T S_1 B' u_3] dV \\
 &= 0
 \end{aligned}
 \tag{35}$$

From equation (35),

$$\begin{aligned}
 d\lambda_c = & - \frac{u_1^T [\int_V B'^T S_4 B' dV] u_1}{u_1^T [\int_V B'^T S_0 B' dV] u_1} \\
 & - \frac{u_1^T [\int_V B'^T S_3 B' dV] u_2}{u_1^T [\int_V B'^T S_0 B' dV] u_1} \\
 & - \frac{u_1^T [\int_V B'^T S_2 B' dV] u_3}{u_1^T [\int_V B'^T S_0 B' dV] u_1} \\
 & - \frac{2u_1^T [\int_V B'^T S_1 B' dV] u_4}{u_1^T [\int_V B'^T S_0 B' dV] u_1} \\
 & - \frac{u_2^T [\int_V B'^T S_1 B' dV] u_3}{u_1^T [\int_V B'^T S_0 B' dV] u_1}
 \end{aligned}
 \tag{36}$$

where S_4 is the matrix with the fourth order stress (σ_4) components similar to S_3 . Postbuckling coefficient d can be calculated using equation (36).

3 Determination of the transition point

The initial postbuckling behavior can be obtained using the Koiter's method, but in order to examine subsequence behavior, it is necessary to conduct the arc-length method. Accordingly, determination of the transition point at which the Koiter's method is switched to the arc-length method is very important. A method that can determine the transition point is derived using the 2nd order and 4th order load parameters written as follow:

$$\begin{aligned}
 \lambda_2 &= 1 + a\xi + b\xi^2 \\
 \lambda_4 &= 1 + a\xi + b\xi^2 + c\xi^3 + d\xi^4
 \end{aligned}
 \tag{37}$$

Because the odd order coefficients such as the first and the third orders, can be "zero" in the case of perfect structures, two even order polynomials is selected.

The relative difference of two different orders of the load parameters can be defined as error tolerance (ER) such that

$$ER = \frac{|\lambda_4 - \lambda_2|}{\lambda_2} = \frac{|c\xi^3 + d\xi^4|}{1 + a\xi + b\xi^2}
 \tag{38}$$

Setting ER to maximum error tolerance ER_m ,

$$\frac{|c\xi_t^3 + d\xi_t^4|}{1 + a\xi_t + b\xi_t^2} = ER_m
 \tag{39}$$

where ξ_t corresponds to ER_m . The transition point ξ_t can be determined from equation (39).

In the case of perfect structures, the odd order coefficient a and c are "zero", and equation (39) can be reduced to

$$\xi_t = \sqrt{\frac{bER_m + \sqrt{(bER_m)^2 + 4|d|ER_m}}{2|d|}}
 \tag{40}$$

In this paper the maximum error tolerance ER_m is set to "0.0001" or "0.01%".

4 Numerical examples

In this paper, an eighteen-node solid shell element as shown in Fig. 2 is used to test Koiter's method combined with the assumed strain formulation for postbuckling analysis. This element has nine nodes on top and

bottom surfaces respectively. There are three degrees of freedom per node. The first three examples are chosen to validate the present approach by comparing with the existing solutions.

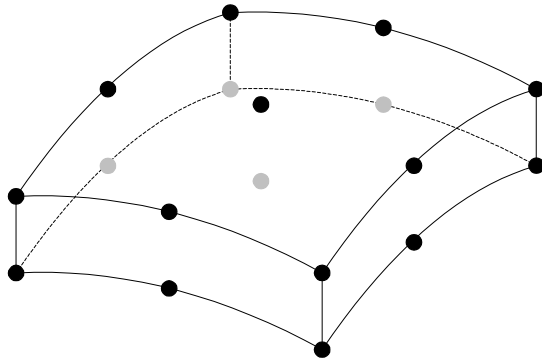


Figure 2 : 18-node solid shell element

4.1 Simply supported slender beam-column

A simply supported slender beam-column under compressive load shown in Fig. 3 is considered. The beam-column is 100m long, 1m wide and thick. The material is isotropic with Young’s modulus $E=2.1 \times 10^{11} Pa$ and Poisson’s ratio $\nu=0$. Half of the beam-column is modeled using fifteen elements. For comparison with the analytical solution, the parameter ξ is defined as the rotation angle at the edge. The results are shown in Tab. 1, and compared with analytical solution [Lanzo, Garcea and Casciaro (1995)]. The postbuckling coefficients obtained by the present method are in good agreement with the analytical values.

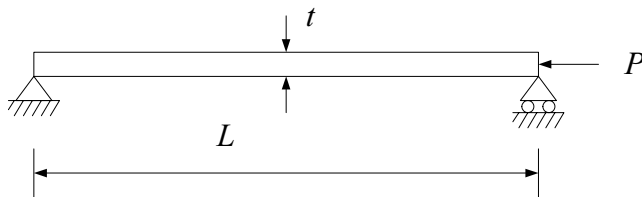


Figure 3 : Simply supported slender beam-column

4.2 Rectangular plate problem

Example A1 is simply supported on all four edges and a compressive load is applied to two opposite edges as

Table 1 : Simply supported slender beam-column

	Present	Analytic
λ_c	1.727×10^7	1.727×10^7
a	0	0
b	0.1247	0.1250

shown in Fig. 4. Example A2 is shown in Fig. 5. The plate width L_y is 100 inch, thickness t is 1 inch and the length varies with the width and aspect ratios. The material is isotropic with Young’s modulus $E=2.1 \times 10^6 psi$ and Poisson’s ratio $\nu=0.25$. The parameter ξ is defined as the maximum out of plane displacement normalized by plate thickness t .

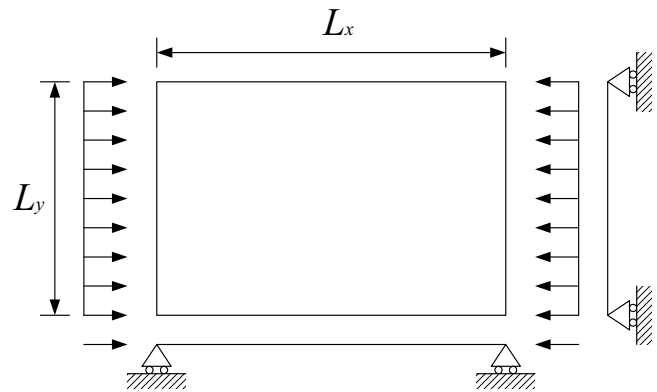


Figure 4 : Example A1

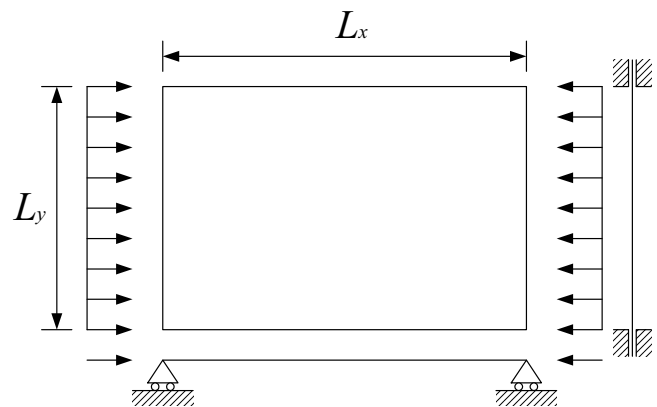


Figure 5 : Example A2

The results of the isotropic rectangular plate problem using present method are compared with Lanzo's results[Lanzo, Garcea and Casciaro (1995)] shown in Tabs. 2 and 3. Lanzo used the high continuity (HC) element based on the von-Karman's nonlinear plate theory. In the tables, the Lanzo's results are listed in parenthesis. The buckling load and the postbuckling coefficients obtained by the present method are in good agreement with the reference solutions.

Table 2 : Example A1 result

	$L_x/L_y=1$ (8×8 mesh)	$L_x/L_y=2$ (17×7 mesh)	$L_x/L_y=3$ (20×7 mesh)
λ_c	7.286 (7.374)	7.304 (7.375)	7.309 (7.382)
b	1.832×10^{-1} (1.824×10^{-1})	2.139×10^{-1} (2.118×10^{-1})	2.228×10^{-1} (2.217×10^{-1})

Table 3 : Example A2 result

	$L_x/L_y=1$ (17×7 mesh)	$L_x/L_y=2$ (20×7 mesh)
λ_c	1.410×10^1 (1.421×10^1)	1.280×10^1 (1.292×10^1)
b	1.972×10^{-1} (1.958×10^{-1})	2.644×10^{-1} (2.654×10^{-1})

4.3 Roorda's frame

Roorda's frame shown in Fig. 6 is solved. Two types of loading conditions are considered. One is the case of $\varphi=0^\circ$ and the other is the case of $\varphi=45^\circ$. The length of each leg is $1m$ and thickness and width are $0.01m$. The material is isotropic with Young's modulus $E=2.1 \times 10^{11} Pa$ and Poisson's ratio $\nu=0$. Two different models are used. In the first model, each leg of the frame is modeled with ten elements as shown in Fig. 7. In the second model, twenty elements are used per each leg. The differences between the two models are less than 0.1%. The parameter ξ is defined as the rotation angle at the loading point. Table 4 shows the results of the second model. In the table, the analytical solutions [Olesen

and Byskov (1982)] are listed in the parentheses. One can observe the buckling load and the postbuckling coefficient a are in good agreement with analytical values. However, the postbuckling coefficient b is different from the analytical solution. This discrepancy is perhaps due to the small angle assumption adopted in the reference solution, while the present solid shell element formulation is free of this limitation.

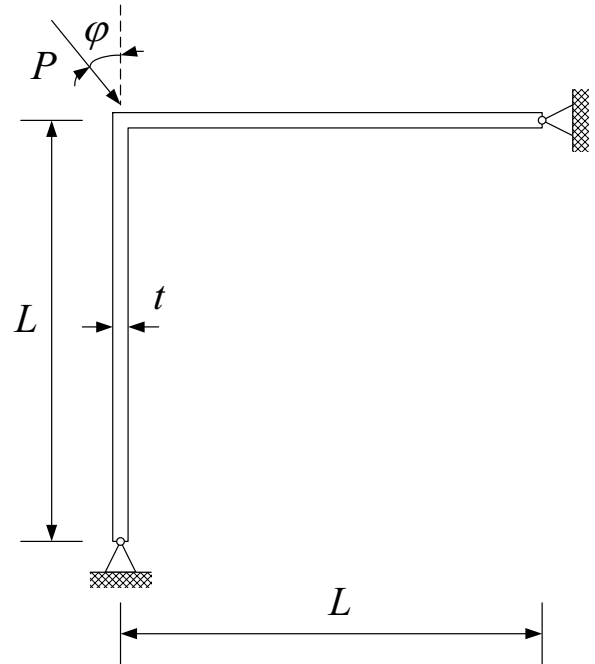


Figure 6 : Roorda's frame

Table 4 : Roorda's frame

	$\varphi=0^\circ$	$\varphi=45^\circ$
λ_c	2.430×10^5 (2.430×10^5)	2.430×10^5 (2.443×10^5)
a	0.3818 (0.3805)	-0.0006 (0)
b	0.3814 (0.1421)	-0.1248 (-0.25)

4.4 Composite plates

The loading and boundary conditions of the composite plates are shown in Fig. 8. The plate length L_x is 100

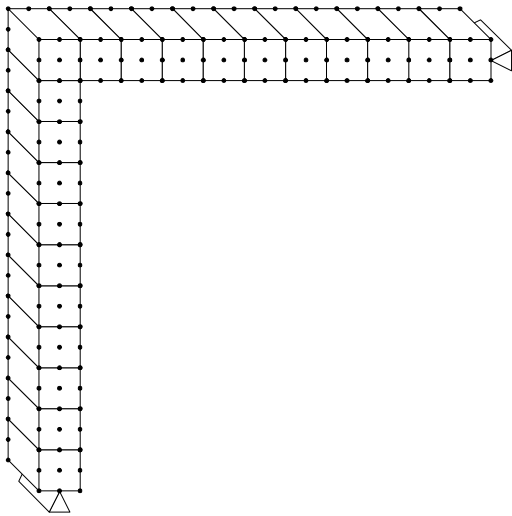


Figure 7 : The model of Roorda’s frame (21 elements)

inch, width L_y is 30 inch and thickness t is 1 inch. Material properties are shown below [Hao, Cho, and Lee (2000)] and composite plate lay-up is $[60/-60/0]_s$.

◇ Graphite/epoxy laminate:

$$E_1=22.48Msi, E_2 = E_3=1.755Msi,$$

$$v_{12}=v_{13}=0.248, v_{23}=0.458,$$

$$G_{12} = G_{31}=0.638Msi, G_{23}=0.464Msi$$

◇ Glass/epoxy laminate:

$$E_1=7.25Msi, E_2 = E_3=2.204Msi,$$

$$v_{12}=v_{13}=0.254, v_{23}=0.428,$$

$$G_{12} = G_{31}=0.6815Msi, G_{23}=0.4756Msi$$

A quarter of plate is modeled with a $4 \times 4 \times 1$ element mesh. The parameter ξ is defined as the maximum out of plane displacement normalized by plate thickness t . The buckling load, the postbuckling coefficients and the transition point of the composite plates are listed in Tab. 5. Figures 9 and 10 show the postbuckling behavior of composite plates. In the vertical axis, applied load P is normalized by buckling load P_{cr} and in the horizontal axis, maximum out of plane displacement w is normalized by plate length L_x . In the figures “Koiter-NL” represents the postbuckling path obtained with the Koiter’s method followed by the arc-length method. The Koiter’s method is used until the transition point at which it is switched to

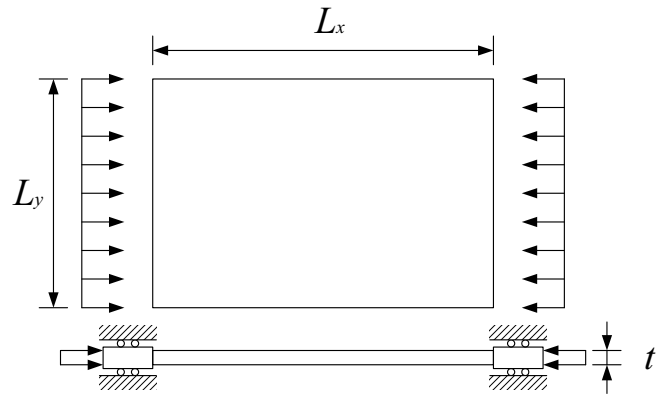


Figure 8 : The composite sandwich plate under uniform compressive load

the arc-length method. The Koiter’s method with a second order expansion is labeled “Koiter_2” while “Koiter_4” represents the Koiter’s method with 4th order expansion. The transition point is also shown in the figure.

Table 5 : Composite plate problems

	Graphite/epoxy laminate	Glass/epoxy laminate
λ_c	2.909×10^4	2.305×10^4
b	6.178×10^{-3}	3.120×10^{-3}
d	-2.627×10^{-4}	-1.209×10^{-4}
ξ_t	0.786	0.954

4.5 Sandwich plates

The loading and boundary conditions of sandwich plates are same as the composite plate shown in Fig. 8. The plate length L_x is 100 inch, width L_y is 30 inch and thickness t is 1 inch. Also, upper skin thickness is 1/12 inch, lower skin thickness is 1/12 inch and core thickness is 10/12 inch. In the case of sandwich plates, composite face sheets lay-up is $[60/-60/0]_s$ and the material properties are identical to those for the composite plates in the previous example. Core properties are shown below [Hao, Cho, and Lee (2000)].

◇ HC (Honeycomb) core:

$$E_1=44.48psi, E_2=40.31psi, E_3=0.556Msi,$$

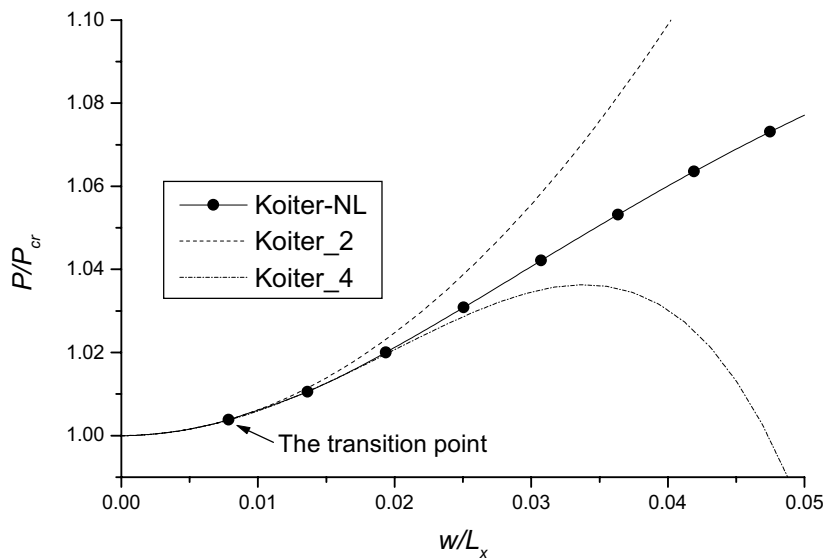


Figure 9 : Graphite/epoxy laminate composite plate

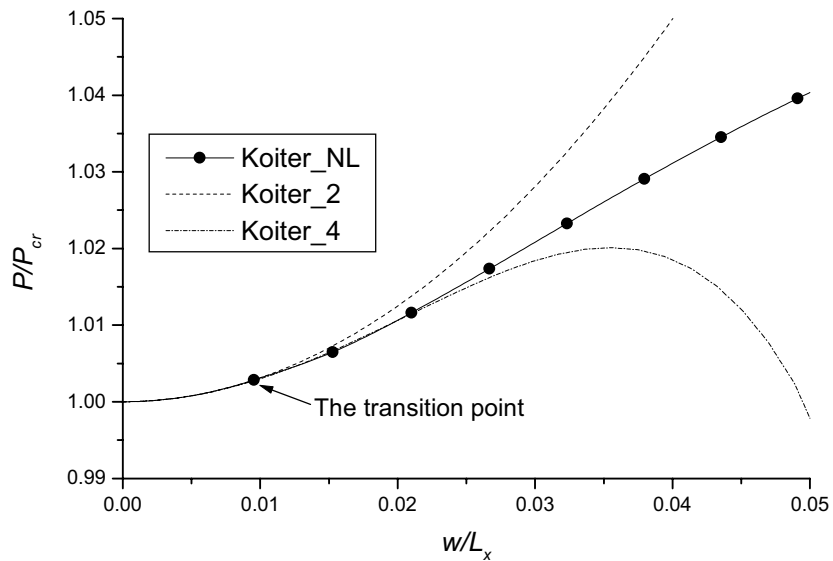


Figure 10 : Glass/epoxy laminate composite plate

$\nu_{12}=0.99, \nu_{23}=0.00003, \nu_{13}=0.00003,$
 $G_{12}=3.36ksi, G_{23}=0.1098Msi, G_{31}=91.74ksi$

$G=14.79ksi$

◇ PVC foam core:

Case 1: $\rho=3.669 \times 10^{-5} slug/in^3 : E=3.915ksi,$
 $G=1.659ksi$

Case 2: $\rho=1.347 \times 10^{-4} slug/in^3 : E=23.91ksi,$
 $G=7.185ksi$

Case 3: $\rho=2.693 \times 10^{-4} slug/in^3 : E=54.52ksi,$

A quarter of plate is modeled with a $4 \times 4 \times 3$ element mesh. Three elements are used through the thickness to model the face sheets and the core separately, with two elements for the face sheets and one element for the core. The parameter ξ is defined as the maximum out of plane displacement normalized by plate thickness t . For the honeycomb core and the foam core of low density (case 1), the buckling loads, the postbuckling coefficients and

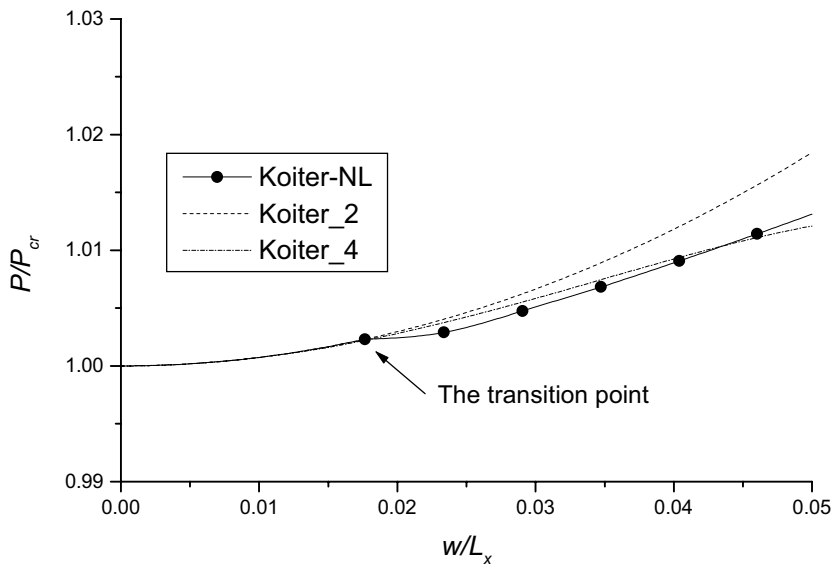


Figure 11 : Graphite/epoxy laminate face sheet and HC core sandwich plate

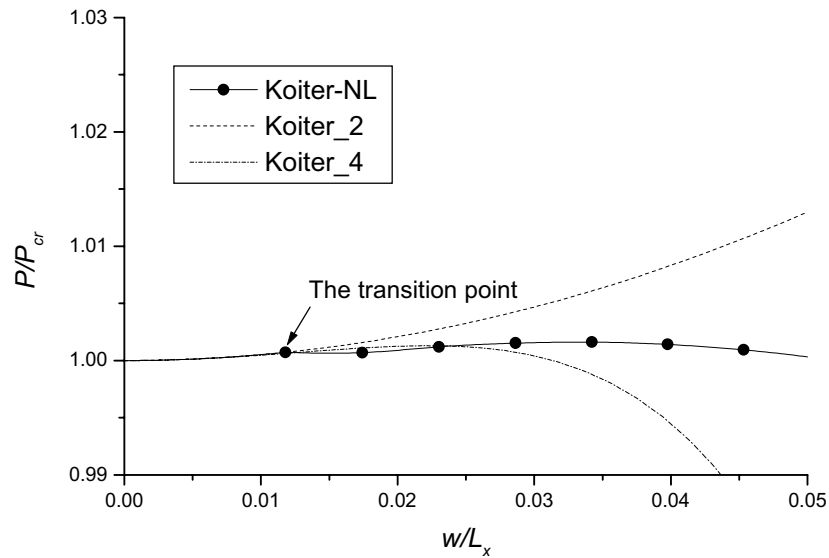


Figure 12 : Graphite/epoxy laminate face sheet and PVC core sandwich plate

the transition point of the sandwich plates are listed in Tabs. 6 and 7. Figures 11-14 show the postbuckling behaviors of the same sandwich plates. Figures 12 and 14 indicate that, for the low density foam core, the postbuckling behavior of the sandwich plate with glass/epoxy face sheets is more stable than that of the plate with graphite/epoxy face sheets.

Also, two other foam cores (Cases 2 and 3) are considered to investigate the effect of core densities on the post-

Table 6 : Graphite/epoxy laminate face sheet sandwich plates

	HCH core	PVC core (Case 1)
λ_c	3.678×10^4	2.100×10^4
b	7.384×10^{-4}	5.197×10^{-4}
d	-1.030×10^{-5}	-5.178×10^{-5}
ξ_t	1.766	1.179

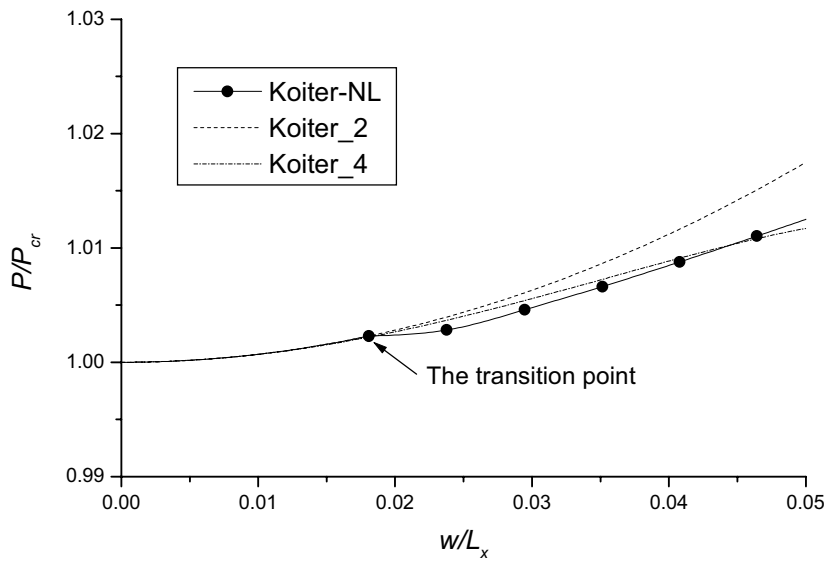


Figure 13 : Glass/epoxy laminate face sheet and HC core sandwich plate

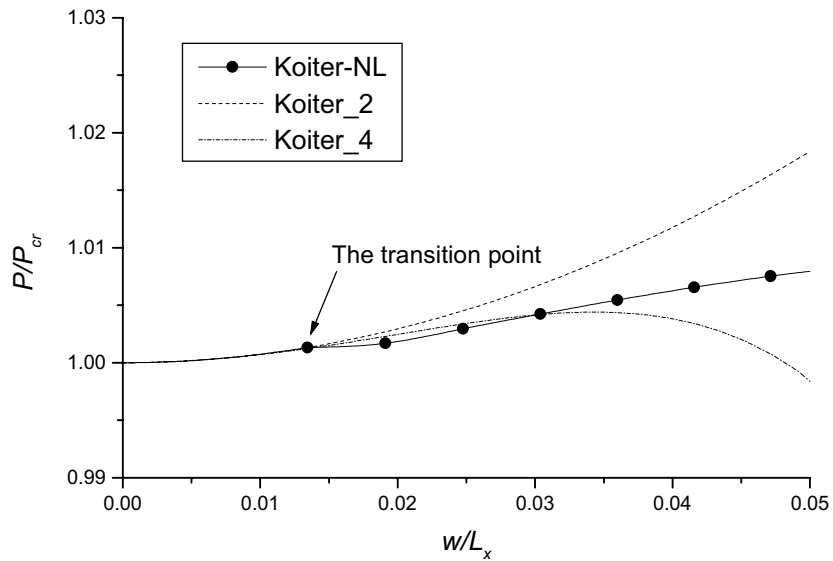


Figure 14 : Glass/epoxy laminate face sheet and PVC core sandwich plate

Table 7 : Glass/epoxy laminate face sheet sandwich plate

	HCH core	PVC core (Case 1)
λ_c	1.598×10^4	1.193×10^4
b	6.996×10^{-4}	7.358×10^{-4}
d	-9.373×10^{-6}	-3.070×10^{-5}
ξ_t	1.808	1.344

buckling behavior. The postbuckling behaviors of the sandwich plates with various core densities are shown in Figs. 15 and 16. One can observe that, as the core density increases, the postbuckling behavior comes to more stable. But the differences between Case 2 and Case 3 are small, especially for the sandwich plates with glass/epoxy face sheets.

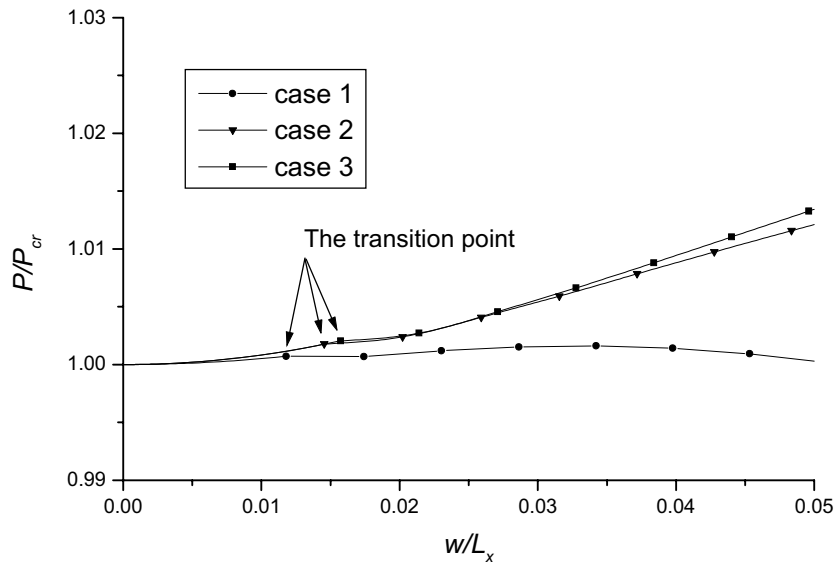


Figure 15 : Graphite/epoxy laminate face sheet and PVC cores with various densities sandwich plate

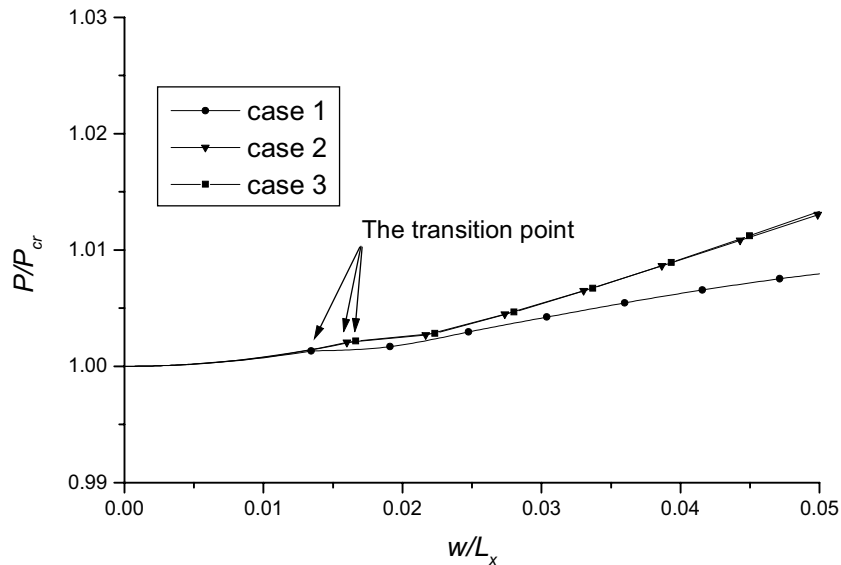


Figure 16 : Glass/epoxy laminate face sheet and PVC cores with various densities sandwich plate

5 Conclusion

In this paper, the assumed strain solid shell element formulation is combined with the Koiter's asymptotic method for postbuckling analysis of composite and sandwich structures. The solid shell element can be easily stacked through the thickness. Accordingly, it is convenient for analysis of sandwich structures with composite face sheets and a core.

The results of the isotropic beam-column and the rectangular plate problems using the present method are in good agreement with the reference solutions. However, in the case of Roorda's frame, the second-order postbuckling coefficient is different from the reference solutions. This discrepancy is perhaps due to the small angle assumption adopted in the reference solution, while the present solid shell element formulation is free of this limitation.

Numerical results demonstrate that, for postbuckling analysis of composite and sandwich structures, the Koiter's method combined with the assumed strain solid shell element formulation can be used to trace initial postbuckling path. Subsequently, the Koiter's method is switched to the arc-length method to investigate postbuckling behavior involving large deflections. The transition point at which the switching occurs is determined using the postbuckling coefficients, obtained from the asymptotic analysis with the fourth order expansion. Numerical results show that, for sandwich plates, the initial postbuckling behavior is stable. However, for plates with a soft core, it can become unstable as the load increases beyond the initial buckling load.

References

- Byskov, E.; Hutchinson, J. W.** (1977): Mode interaction in axially stiffened cylindrical shells. *AIAA Journal*, Vol. 15, No. 7.
- Byskov, E.** (1989): Smooth postbuckling stresses by a modified finite element method. *IJNME*, Vol. 28, pp. 2877-2888.
- Byskov, E.; Christensen, C. D.; Jorgensen, K.** (1996): Elastic postbuckling with nonlinear constraints. *Int. J. Solids Structures*, Vol. 33, No. 17, pp. 2417-2436.
- Casciaro, R.; Salerno, G.; Lanzo, A. D.** (1992): Finite element asymptotic analysis of slender elastic structures: a simple approach. *IJNME*, Vol. 35, pp. 1397-1426.
- Casciaro, R.; Garcea, G.; Attanasio, G.; Giordano, F.** (1998): Perturbation approach to elastic post-buckling analysis. *Computers & Structures*, Vol. 66, No. 5, pp. 585-595.
- Clarke, M. J.; Hancock, G. J.** (1990): A study of incremental-iterative strategies for non-linear analysis. *IJNME*, Vol. 29, pp. 1365-1391.
- Garcea, G.; Salerno, G.; Casciaro, R.** (1999): Extrapolation locking and its sanitization in Koiter's asymptotic analysis. *Computer Methods in Applied Mechanics and Engineering*, Vol. 180, pp. 137-167.
- Garcea, G.** (2001): Mixed formulation in Koiter analysis of thin-walled beams. *Computer Methods in Applied Mechanics and Engineering*, Vol. 190, pp. 3369-3399.
- Glaessgen, E. H.; Riddell, W. T.; Raju I. S.** (2002): Nodal constraint, shear deformation and continuity effects related to the modeling of debonding of laminates, using plate elements. *CMES: Computer Modeling in Engineering & Sciences*, Vol. 3, No. 1, pp. 103-116.
- Hao, B.; Cho, C.; Lee, S. W.** (2000): Buckling and post-buckling of soft-core sandwich plates with composite facesheets. *Computational Mechanics*, vol. 25, no. 5, pp. 421-429.
- Kim, Y. H.; Lee, S. W.** (1988): A solid element formulation for large deflection analysis of composite shell structures. *Comput. Struct.*, 30, 269-274.
- Lanzo, A. D.; Garcea, G.; Casciaro, R.** (1995): Asymptotic post-buckling analysis of rectangular plates by HC finite elements. *IJNME*, Vol. 38, pp. 2325-2345.
- Lanzo, A. D.; Garcea, G.** (1996): Koiter's analysis of thin-walled structures by a finite element approach. *IJNME*, Vol. 39, 3007-3031.
- Lanzo, A. D.** (2000): A Koiter's perturbation strategy for the imperfection sensitivity analysis of thin-walled structures with residual stresses. *Thin-Walled Structures*, Vol. 37, pp. 77-95.
- Lee, K.; Cho, C.; Lee, S. W.** (2002): A geometrically nonlinear nine-node solid shell element formulation with reduced sensitivity to mesh distortion. *CMES: Computer Modeling in Engineering & Sciences*, Vol. 3, No. 3, pp. 339-350.
- Olesen, J. F.; Byskov, E.** (1982): Accurate determination of asymptotic postbuckling stresses by the finite element method. *Computers & Structures*, Vol. 15, No. 2, pp. 157-163.
- Poulsen, P. N.; Damkilde, L.** (1998): Direct determination of asymptotic structural postbuckling behaviour by the finite element method. *IJNME*, Vol. 42, pp. 685-702.
- Salerno, G.; Lanzo, A. D.** (1997): A nonlinear beam finite element for the post-buckling analysis of plane frames by Koiter's perturbation approach. *Computer Methods in Applied Mechanics and Engineering*, Vol. 146, pp. 325-349.